Thermochimica Acta 512 (2011) 71–75

Contents lists available at ScienceDirect

Thermochimica Acta

journal homepage: www.elsevier.com/locate/tca

Studies of irreversible heat denaturation of green fluorescent protein by differential scanning microcalorimetry

Tatiana Melnik, Tatiana Povarnitsyna, Helena Solonenko, Bogdan Melnik*

Institute of Protein Research, RAS, 142290 Pushchino, Moscow Region, Russia

ARTICLE INFO

Article history:
Received 6 April 2010
Received in revised form 1 September 2010
Accepted 2 September 2010
Available online 15 September 2010

Keywords:
Green fluorescent protein
Irreversible denaturation
Transition state

ABSTRACT

Heat denaturation of green fluorescent protein (the GFP-cycle3 mutant) was studied by the method of differential scanning microcalorimetry. Activation energy values for two stages of GFP unfolding were calculated from the calorimetric data using the model of irreversible denaturation. Dependences of activation energy and denaturation enthalpy on the temperature of the maxima of corresponding stages of denaturation were obtained, which allow estimating the corresponding increments of heat capacity. Based on the known correlations of the structure and energy parameters, it was concluded that the first transition state is close to the native state, whereas the second transition state is close to the denatured state, judging by the exposure of hydrophobic groups to the solvent.

1. Introduction

Microcalorimetry is a traditional technique for studying proteins whose melting is equilibrium and reversible. For such a research, mathematical methods have been developed which permit obtaining important thermodynamic data from experimental heat absorption curves [1]. However, in many cases it is impossible to achieve equilibrium conditions in calorimetric measurements. It is for such cases that mathematical methods of analysis of the melting curves have been designed [2–6] allowing one to calculate the activation energy and rate constants of unfolding for a protein at its irreversible and non-equilibrium melting. Thus non-equilibrium melting of protein permits receiving information on its transition states, i.e. the states that determine the size of barriers between stable states of the protein. In this work, the method of differential scanning microcalorimetry is used to study non-equilibrium melting of the mutant green fluorescent protein cycle-3 (GFP- cycle3) from *Aequorea victoria* [7,8]. GFP is a soluble globular protein that looks like a beta-barrel with an alpha-helix within it. In the middle of the helix, the chromophore is formed in an autocatalytic manner. In numerous studies GFP is used as a biosensor for protein–protein interactions, co-translational folding and localization of different structures in cells [9,10]. However, there are only few investigations in which stability and folding of GFP per se are analyzed. This protein is quite a complex object for such studies which may be explained by the formation and disruption of its native structure in vitro proceeding in several rather prolonged stages, during which the protein is not stable and undergoes aggregation [11,12]. The protein has been studied mostly by optical methods such as fluorescence of tryptophane residues, fluorescence of GFP chromophore and circular dichroism which permit measuring the kinetics of folding/unfolding and calculating rate constants, but unfortunately these methods do not yield any information on structural peculiarities of activated (transition) states of the protein [11,13–15]. We conducted a microcalorimetric study of thermal unfolding of GFP-cycle3 under conditions when its melting is non-equilibrium. In addition, the analysis of the dependences of activation energy and denaturation enthalpy versus the temperature of maxima of corresponding stages of denaturation allowed us to get information on the extent of hydration of hydrophobic groups of two transition states at unfolding of GFP-cycle3.

2. Materials and methods

2.1. Protein expression and isolation

The plasmid containing the gene of GFP-cycle3 (pBAD-GFP-cycle3 produced by Maxygen) was expressed in *E. coli* BL21(DE3) cells. The protein was prepared and isolated as described elsewhere [11]. The purity of the isolated protein was checked by SDS-electrophoresis in polyacrylamide gel. The ratio of the absorbance at 395 nm to that at 280 nm, which is an index of purity of GFP, is 1.1–1.2 for pure GFP [16]. The final sample prepared had the ratio of 1.1 or higher. The protein concentration was determined by UV absorption at 280 nm with the extinction coefficient $A_{280}^{0.1\%} = 0.77$ [11].

* Corresponding author at: Institute of Protein Research (Moscow Office), Room 104, Vavilova Street 34, Moscow, GSP 1, 117334, Russia. Tel.: +7 495 514 02 18; fax: +7 499 135 2147.
E-mail address: bmelnik@phys.protres.ru (B. Melnik).

0040-6031/$ – see front matter © 2010 Elsevier B.V. All rights reserved.
doi:10.1016/j.tca.2010.09.002

2.2. Calorimetric measurements

Calorimetric measurements were made on a precision scanning microcalorimeter SCAL-1 (Scal Co., Ltd., Russia) with 0.33 ml glass cells [17] at a scanning rate of 0.25, 0.5, 1 K/min and under the pressure of 2.5 atm. The experiments were performed between 0 and 100 °C in 25 mM sodium phosphate buffer at pH 5.6–7.3. The protein concentrations in the experiment varied from 0.5 mg/ml to 5.0 mg/ml. In this concentration range, the kinetic and thermodynamic parameters remained stable. The experimental calorimetric profiles were corrected for the calorimetric baseline, and the molar partial heat capacity functions were calculated in a standard manner. The excess heat capacity was evaluated by subtracting the linearly extrapolated initial and final heat capacity functions with correction for the difference of these functions by using a sigmoid baseline [1]. A typical value for the partial specific volume for globular proteins (0.73 cm^3/g) was accepted arbitrarily, since it does not influence the calculated excess heat capacity.

,

2.3. The two-step models for the irreversible thermal denaturation

The curves of the dependence of excess heat capacity versus temperature were analyzed using the following models for the protein denaturation. The Lumry–Eyring model with the fast equilibrating first step, in which folding and unfolding rate constants (k_1, k_{-1}) of the first step is high in comparison with k of the second step, can be represented by the following scheme:

$$\mathrm{N} \underset{k_{-1}}{\overset{k_1}{\underset{(K)}{\rightleftarrows}}} \mathrm{I} \xrightarrow{k} \mathrm{D} \quad (1)$$

where N, I and D are the native, intermediate and denatured states of the protein, respectively. K is the equilibrium constant for the first step. The excess heat capacity C_p^{exc} versus absolute temperature (T) is calculated from the equation [18]:

$$C_p^{exc} = \left[\frac{\Delta H_u K}{(K+1)^2}\left(\frac{k}{\nu}+\frac{\Delta H_u}{RT^2}\right)+\Delta H_i \frac{1}{\nu}\frac{kK}{K+1}\right] \exp\left(-\frac{1}{\nu}\int_{T_0}^{T}\frac{kK}{K+1}\,dT\right) \quad (2)$$

where ΔH_u and ΔH_i are the changes of enthalpy associated with the first and second steps, respectively. $\nu = dT/dt$ is the scanning rate. T is the absolute temperature and T_0 is the temperature of the beginning of the heat absorption curve. K is the equilibrium constant for the first step that can be expressed as:

$$K = \exp\left[\frac{-\Delta H_u}{R(1/T - 1/T_{1/2})}\right] \quad (3)$$

k is the rate constant for the second step that can be expressed as:

$$k = \exp\left[\frac{-\Delta E^{\#}}{R(1/T - 1/T^*)}\right] \quad (4)$$

where $\Delta E^{\#}$ is the energy of activation for the second process, $T_{1/2}$ is the temperature at which $K = 1$, T^* is a temperature parameter equal to the temperature at which $k = 1\ \mathrm{min}^{-1}$.

The other model of irreversible denaturation is a model involving two consecutive irreversible steps of denaturation:

$$\mathrm{N} \xrightarrow{k_1} \mathrm{I} \xrightarrow{k_2} \mathrm{D} \quad (5)$$

The equation for C_p^{exc} describing this model is as follows [3]:

$$C_p^{exc} = \frac{\Delta H_1 k_1}{\nu}\exp\left(-\frac{1}{\nu}\int_{T_0}^{T} k_1\,dT\right)+\frac{\Delta H_2 k_2}{\nu^2}\exp\left(-\frac{1}{\nu}\int_{T_0}^{T} k_1\,dT\right) \times \int_{T_0}^{T}\left[k_1 \exp\left(\frac{1}{\nu}\int_{T_0}^{T}(k_2-k_1)\,dT\right)\right] dT \quad (6)$$

where ΔH_1 and ΔH_2 are changes of enthalpy for the first and second steps, k_1 and k_2 are rate constants for the first and second steps:

$$k_1 = \exp\left[\frac{-\Delta E_1^{\#}}{R(1/T - 1/T_1^*)}\right] \quad \text{and} \quad k_2 = \exp\left[\frac{-\Delta E_2^{\#}}{R(1/T - 1/T_2^*)}\right] \quad (7)$$

On the basis of Eqs. (2) and (6), the experimental profiles of GFP-cycle3 denaturation were fitted by the IgorPro program (WaveMetrics, Inc.,), and the activation energies $\Delta E_1^{\#}$, $\Delta E_2^{\#}$ were determined.

3. Results and discussion

3.1. Calorimetric melting of GFP-cycle3

Fig. 1 shows melting curves of GFP-cycle3. It can be seen that the position and the shape of the heat absorption peak change remarkably dependent on the heating rate. This suggests that the protein melting in the range of selected heating rates is a non-equilibrium process. In other words, denaturation at the given conditions is either irreversible basically, or the heating rates are too high for the process to be equilibrium. As demonstrated earlier, the both cases do not differ in the shape of melting curves [19,20]. The criterion given in [2] allows analyzing quite easily whether this non-equilibrium denaturation of the studied protein proceeds in one or several steps. To this end, it is required to plot experimental melting curves in the ($\ln[\nu C_p/(\Delta H - Q)]$; $1/T$) coordinates where ν is the rate of heating the sample in the calorimeter, C_p is the value of excess thermal capacity at the given temperature, ΔH is the enthalpy (estimated as the integral of the complete experimental melting curve), and Q is the heat absorbed upon denaturation (estimated as the integral of the experimental melting curve from its beginning through the current temperature value). In case the protein denaturation is a one-stage mechanism, the experimental

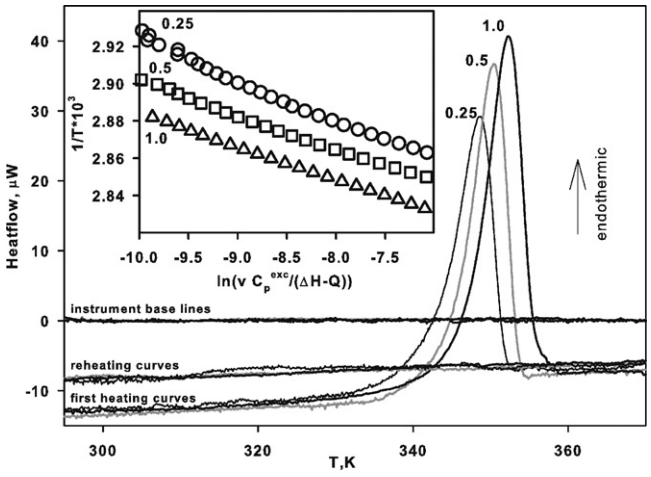

Fig. 1. DSC curves of the first heating and reheating of 0.15% GFP-cycle3 solution at pH 6.2 and instrument base lines measured at three heating rates (1.0, 0.5, 0.25 K/min). Symbols (○, □, △) in the insert show experimental melting data in coordinates $1/T$ versus $\ln[\nu C_p/(\Delta H - Q)]$. The discrepancy of the curves in these coordinates demonstrates that heat denaturation of GFP-cycle3 cannot be described by a one-stage model.

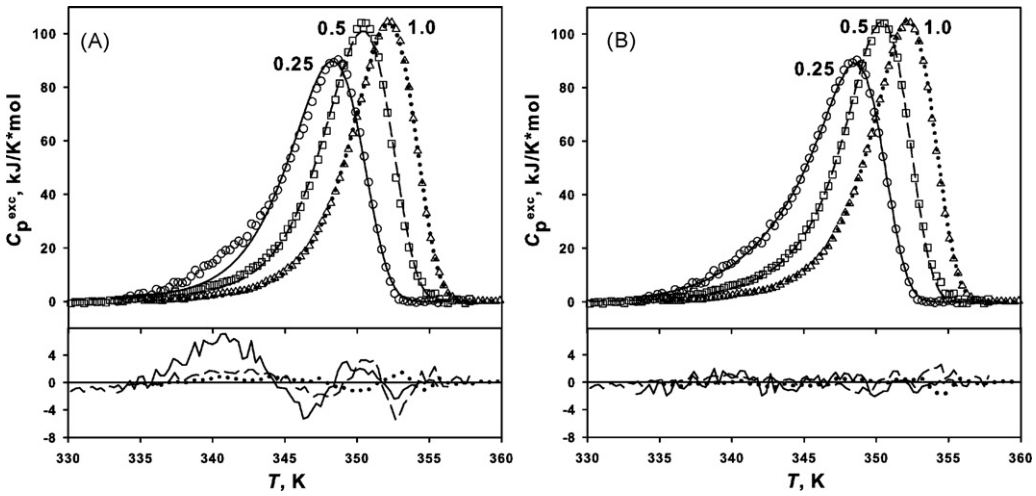

Fig. 2. Temperature dependences of excess heat capacity functions for GFP-cycle3 at pH 6.2 measured at three heating rates (0.25, 0.5, 1.0 K/min). Symbols (○, □, △) show experimental data, and lines (—, – – –, ···) show the best fit of the experimental data using the Lumry–Eyring model with fast equilibrating first step A and the model with two consecutive irreversible steps B. Curves at the lower plots are residual ones.

heat absorption curves plotted in these coordinates should be independent of the heating rate of the calorimeter (i.e. they should be compatible). In the insert of Fig. 1, curves of the GFP-cycle3 melting measured at three heating rates (0.25, 0.5 and 1.0 K/min) are plotted in such coordinates. It is apparent that the experimental curves are not concurrent in these coordinates. This means that heat denaturation of GFP-cycle3 cannot be described by the one-stage model. Therefore it is necessary to use a more complex model of irreversible denaturation.

The Lumry–Eyring model [3,18,19] is the most attractive model for protein denaturation. It involves a reversible unfolding step followed by an irreversible denaturation step:

$$\mathrm{N} \underset{k_{-1}}{\overset{k_1}{\rightleftarrows}} \mathrm{I} \xrightarrow{k_2} \mathrm{D} \qquad (8)$$

where N, I and D are the native, intermediate and denatured states of the protein, respectively. It should be noted that the system of differential equations describing the whole kinetic Lumry–Eyring model has no analytical solution at varying temperature. This circumstance hampers using the model. Two specific cases of the whole kinetic Lumry–Eyring model are the following more simple two-step models: the Lumry–Eyring model with a fast equilibrating first step and the model involving two consecutive irreversible steps [3,18].

In Fig. 2A experimentally obtained dependences of the excess partial heat capacity of GFP-cycle3 versus temperature at pH 6.2 are shown by symbols, while their fitting by the Lumry–Eyring model with the fast equilibrating first step is shown by lines (Eq. (2)). The parameters of the fitting are given in Table 1. To raise the accuracy of estimations for the three melting curves, combined fitting was performed because the curves reproduce the transition between the same three states and, consequently, they should be described by equations with both the same activation energy $\Delta E^{\#}$ and temperatures $T_{1/2}$ and T^* (Eqs. (3) and (4)). The curves at the lower plots in Fig. 2A are residual ones. It is evident that the calculated curves give a poor description of the experimental data. The greatest differences are observed between the theoretically calculated curve and the experimental one obtained at the heating rate of 0.25 K/min. Such a divergence demonstrates that the model of denaturation for the description of these melting peaks is not adequate in this case.

Fig. 1B shows combined fitting of the experimental curves with the same $\Delta E_1^{\#}$, T_1^*, $\Delta E_2^{\#}$, and T_2^* values for the three curves in Eqs. (6) and (7) using the model with two consecutive irreversible stages of denaturation. It is apparent that the theoretically calculated curves describe experimental observations perfectly. The results of fitting Eqs. (6) and (7) to the experimental data are shown in Table 1. To make certain that the kinetic parameters obtained from the calorimetric data are really relevant to the phases of GFP-cycle3 unfolding, we performed a kinetic experiment using fluorescence of the chromophore excited at 400 nm. The unfolding reactions were induced by temperature jumps from the native state at T = 293 K, pH 6.2 in a 25 mM phosphate buffer solution to various T values which are characteristic of the denaturation range in the same buffer. The kinetic curves were well fitted to two exponents, which allowed estimating two rate constants of GFP-cycle3 unfolding in the temperature range from 346 K to 353 K. Kinetic parameters obtained

Table 1
Combined fitting parameters estimate for heat denaturation of GFP-cycle3 at pH 6.2.

Model with the fast equilibrating first step (Eq. (1))					
Scanning rate (K/min)	$\Delta H_u \pm 5$ (kJ/mol)	$\Delta H_i \pm 6$ (kJ/mol)	$T_{1/2} \pm 0.2$ (K)	$\Delta E^{\#} \pm 2$ (kJ/mol)	$T^* \pm 0.1$ (K)
0.25	102	522			
0.5	167	492	352.9	344	365.1
1	321	297			

Model with two consecutive irreversible steps (Eq. (5))						
Scanning rate (K/min)	$\Delta H_1 \pm 5$ (kJ/mol)	$\Delta H_2 \pm 6$ (kJ/mol)	$\Delta E_1^{\#} \pm 4$ (kJ/mol)	$\Delta E_2^{\#} \pm 2$ (kJ/mol)	$\Delta T_1^* \pm 0.2$ (K)	$\Delta T_2^* \pm 0.1$ (K)
0.25	201	440				
0.5	136	513	311	438	366.4	363.8
1	124	502				

Table 2
Experimental and fitting parameters of heat denaturation of GFP-cycle3 at diferent pH and scan rate 1 K/min.

Experimental data			Fitting parameters (using Eq. (2) for two consecutive irreversible stages)					
$T_{max} \pm 0.2$ (K)	pH ± 0.1	$\Delta H_d \pm 50$ (kJ/mol)	ΔH_1 (kJ/mol)	ΔH_2 (kJ/mol)	$\Delta E_1^{\#}$ (kJ/mol)	$\Delta E_2^{\#}$ (kJ/mol)	T_1^* (K)	T_2^* (K)
348.5	5.5	513	181	336	372	443	345.2	359.7
348.6	5.6	571	214	356	260	448	345.3	359.8
349.5	5.65	524	257	266	399	446	346.4	360.6
349.9	5.8	552	228	325	366	412	346.9	361.4
350.4	5.85	593	240	348	419	455	347.5	361.2
351.1	5.9	503	183	320	401	412	348.3	362.7
351.6	6.0	524	231	293	434	444	348.9	362.6
352.2	6.2	624	124	502	**311**	**438**	**366.4**	**363.8**
352.4	6.25	573	246	325	421	445	349.9	363.3
352.6	6.3	625	207	421	388	474	350.1	361.9
352.9	6.4	648	275	372	328	442	350.4	361.9
353.8	6.5	642	252	386	282	468	351.5	364.7
354.5	6.6	632	216	415	333	506	352.4	363.9
354.8	6.7	589	260	334	416	519	352.7	364.7
354.9	6.75	604	189	417	432	494	352.9	363.1
356.2	7.0	628	199	429	432	538	354.4	364.6
356.5	7.2	638	256	377	**315**	**471**	**372.8**	**367.3**
356.6	7.3	694	183	513	425	541	354.8	364.3

T_{max} is the temperature of the maximum of the experimental heat absorption curve. Parameters $\Delta E_1^{\#}$, $\Delta E_2^{\#}$, T_1^*, and T_2^* at pH 6.2 and 7.2 (highlighted bold) were obtained at combined fitting of melting curves at three rates (0.25, 0.5 and 1.0 K/min).

from calorimetric experiments (see Eq. (7)) and those from kinetic experiments agree well (data not shown).

Hence, in the first place we have determined that the measured heat absorption peaks can yield information on two stages of GFP-cycle3 denaturation and can be described by a model with two consecutive irreversible steps of denaturation, and second, we have calculated two values of activation energy which permits us to get information on transition states of GFP-cycle3.

3.2. Structural characteristics of transition states of GFP-cycle3

Having ascertained that the model with two consecutive irreversible stages of denaturation can be used for a reliable description of experimental data and for calculation of the activation energy of GFP-cycle3, we applied the calorimetric approach for the analysis of transition states of the protein.

We performed several experiments of GFP-cycle3 melting at different pH with the heating rate of 1 K/min. pH was varied from 5.6 to 7.3, the temperature of the melting peak maximum being changed from 348.5 K to 356.6 K. The melting profile of every curve of the dependence of excess heat capacity versus temperature was fitted using Eq. (6), which describes the model with two consecutive irreversible stages of denaturation. The experimental and the calculated data are summarized in Table 2. As a result, two activation energy values $\Delta E_1^{\#}$ and $\Delta E_2^{\#}$ were calculated from every melting curve (see Table 2). The denaturation enthalpy ΔH_d was estimated directly from the experimental curves in the range of 330–360 K. Fig. 3A shows dependences of two activation energies of denaturation $\Delta E_1^{\#}$ and $\Delta E_2^{\#}$ and the denaturation enthalpy ΔH_d versus the temperature of the corresponding melting peaks maxima. On the basis of the transition-state theory, the activation energy, $\Delta E^{\#}$, can in fact be considered as the activation enthalpy, $\Delta H^{\#}$, since they differ by RT (≅2.7 kJ/mol), i.e. a value which is close to our experimental error. It is known that the denaturation enthalpy of proteins is practically independent of pH [21] and is a function of the temperature only. Abnormal titration of groups that can occur at denaturation does not contribute noticeably to the denaturation enthalpy, at least at the acidic and neutral pH. The same assumption may be also taken for the activation energy [18,22–24]. These considerations suggest that the slope of the dependencies given in Fig. 3A should coincide with the corresponding heat capacity increments (ΔC_p^{den}, $\Delta C_{p1}^{\#}$, $\Delta C_{p2}^{\#}$) [21]. Their values are 16 ± 4 J/(K mol) for denaturation, and 3 ± 4 and 12 ± 2 kJ/(K mol) for the first stage activation and for the second stage activation, respec-

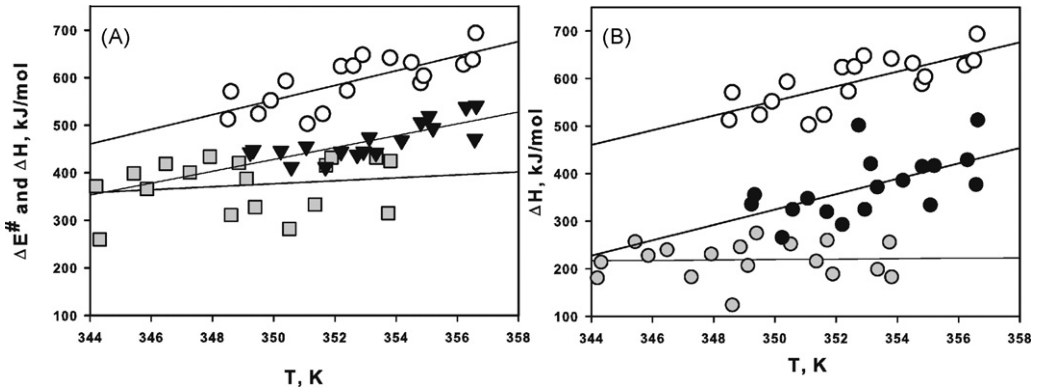

Fig. 3. Dependences of enthalpy and activation energies of denaturation versus the temperature of maxima of corresponding stages of denaturation. The temperatures of maxima of every denaturation stage are estimated theoretically by decomposing the experimental melting peak in constituents by using the model with two consecutive irreversible steps (according to [27]). Activation energies $\Delta E_1^{\#}$ (■) and $\Delta E_2^{\#}$ (▼) of the first and second transitions are shown in panel A. Enthalpies ΔH_1 (○) and ΔH_2 (●) of the first and second transitions are shown in panel B. Denaturation enthalpy ΔH_d (○) is shown in both panels. Lines illustrate approximation of these dependences by the least squares method and the slope of the dependences corresponds to the heat capacity increments $\Delta C_{p1}^{\#} = 3 \pm 4$ kJ/(K mol), $\Delta C_{p2}^{\#} = 12 \pm 2$ kJ/(K mol), $\Delta C_{p1}^{den} = 0 \pm 5$ kJ/(K mol), $\Delta C_{p2}^{den} = 16 \pm 5$ kJ/(K mol) and $\Delta C_p^{den} = 16 \pm 5$ kJ/(K mol).

tively. Fig. 3B demonstrates dependences of the first-transition and second-transition enthalpies (ΔH_1, ΔH_2) versus the temperature of maxima of an appropriate transition, calculated when fitting the experimental curves by the model of Eq. (5). As seen from Table 2, the sums of ΔH_1 and ΔH_2 are compatible with the ΔH_d values measured experimentally, which confirms good fitting of all experimental curves. The above data allowed us to estimate the heat capacity jumps of transitions from the native state to the intermediate one ($\Delta C_{p1}^{\#} = 0 \pm 5$ kJ/(K mol)) and from the intermediate state to the denatured one ($\Delta C_{p2}^{\#} = 16 \pm 5$ kJ/(K mol)).

It was shown previously that the heat capacity increment correlates well with the exposure of the hydrophobic surface during conformational transition [25]. Therefore it can be proposed that by the extent of exposure of hydrophobic groups, the first transition and intermediate states of GFP-cycle3 are close to the native state, i.e. they are compact states with a somewhat hydrated hydrophobic core. In addition, it is likely that the energy barrier between the native and intermediate states exists due to the requirement to destroy some short-living interactions within the protein molecule. The heat capacity increment of the second transition (activated) state ($\Delta C_{p2}^{\#}$) is close in its magnitude to the denaturation heat capacity increment, i.e. the second transition state is less compact and is close to the denatured state by the extent of exposure of hydrophobic groups. At the same time it should be noted that this transition state is quite structured because it is characterized by large activation energy $\Delta E_2^{\#}$ which is an enthalpy component of the energy barrier [26].

4. Conclusions

Heat denaturation of GFP-cycle3 can be described by using a model of two consecutive irreversible stages of denaturation. Two transition states during heat unfolding of GFP-cycle3 were characterized. The first transition state is hydrated almost to the same extent as the native state, i.e. its compactness and structure are quite close to those of the native state of GFP-cycle3. On the contrary, the extent of hydration of hydrophobic groups of the second transition state is close to the hydration of the denatured GFP-cycle3, which shows that practically all hydrophobic interactions in this state are destroyed.

Acknowledgments

The authors are grateful to Dr. S.A. Potekhin for reading the manuscript and fruitful discussion. This work was supported in part by the MCB program of the Russian Academy of Sciences, a “Scientific Schools” grant and the Special Federal Program “Research and Scientific-Pedagogical Specialists of Innovation Russia” (P304).

References

[1] P.L. Privalov, S.A. Potekhin, Scanning microcalorimetry in studying temperature-induced changes in proteins, Methods Enzymol. 131 (1986) 4–51.
[2] B.I. Kurganov, A.E. Lyubarev, J.M. Sanchez-Ruiz, V.L. Shnyrov, Analysis of differential scanning calorimetry data for proteins. Criteria of validity of one-step mechanism of irreversible protein denaturation, Biophys. Chem. 69 (1997) 125–135.
[3] A.E. Lyubarev, B.I. Kurganov, A.A. Burlakova, V.N. Orlov, Irreversible thermal denaturation of uridine phosphorylase from *Escherichia coli* K-12, Biophys. Chem. 70 (1998) 247–257.
[4] A.E. Lyubarev, B.I. Kurganov, V.N. Orlov, H.M. Zhou, Two-state irreversible thermal denaturation of muscle creatine kinase, Biophys. Chem. 79 (1999) 199–204.
[5] S.A. Potekhin, E.L. Kovrigin, Influence of kinetic factors on heat denaturation and renaturation of biopolymers, Biofizika 43 (1998) 223–232.
[6] J.M. Sanchez-Ruiz, J.L. Lopez-Lacomba, M. Cortijo, P.L. Mateo, Differential scanning calorimetry of the irreversible thermal denaturation of thermolysin, Biochemistry 27 (1988) 1648–1652.
[7] R. Battistutta, A. Negro, G. Zanotti, Crystal structure and refolding properties of the mutant F99S/M153T/V163A of the green fluorescent protein, Proteins 41 (2000) 429–437.
[8] M. Ormo, A.B. Cubitt, K. Kallio, L.A. Gross, R.Y. Tsien, S.J. Remington, Crystal structure of the *Aequorea victoria* green fluorescent protein, Science 273 (1996) 1392–1395.
[9] N.C. Shaner, P.A. Steinbach, R.Y. Tsien, A guide to choosing fluorescent proteins, Nat. Methods 2 (2005) 905–909.
[10] R.Y. Tsien, The green fluorescent protein, Annu. Rev. Biochem. 67 (1998) 509–544.
[11] H. Fukuda, M. Arai, K. Kuwajima, Folding of green fluorescent protein and the cycle3 mutant, Biochemistry 39 (2000) 12025–12032.
[12] B.S. Melnik, T.V. Povarnitsyna, T.N. Melnik, Can the fluorescence of green fluorescent protein chromophore be related directly to the nativity of protein structure? Biochem. Biophys. Res. Commun. 390 (2009) 1167–1170.
[13] B.T. Andrews, A.R. Schoenfish, M. Roy, G. Waldo, P.A. Jennings, The rough energy landscape of superfolder GFP is linked to the chromophore, J. Mol. Biol. 373 (2007) 476–490.
[14] S. Enoki, K. Saeki, K. Maki, K. Kuwajima, Acid denaturation and refolding of green fluorescent protein, Biochemistry 43 (2004) 14238–14248.
[15] O.V. Stepanenko, V.V. Verkhusha, V.I. Kazakov, M.M. Shavlovsky, I.M. Kuznetsova, V.N. Uversky, K.K. Turoverov, Comparative studies on the structure and stability of fluorescent proteins EGFP, zFP506, mRFP1, “dimer2”, and DsRed1, Biochemistry 43 (2004) 14913–14923.
[16] W.W. Ward, S.H. Bokman, Reversible denaturation of Aequorea green-fluorescent protein: physical separation and characterization of the renatured protein, Biochemistry 21 (1982) 4535–4540.
[17] A.A. Senin, S.A. Potekhin, E.I. Tiktopulo, V.V. Filomonov, Differential scanning microcalorimetr SCAL-1, J. Therm. Anal. Calorim. 62 (2000) 153–160.
[18] D. Milardi, R.C. La, D. Grasso, Extended theoretical analysis of irreversible protein thermal unfolding, Biophys. Chem. 52 (1994) 183–189.
[19] J.R. Lepock, K.P. Ritchie, M.C. Kolios, A.M. Rodahl, K.A. Heinz, J. Kruuv, Influence of transition rates and scan rate on kinetic simulations of differential scanning calorimetry profiles of reversible and irreversible protein denaturation, Biochemistry 31 (1992) 12706–12712.
[20] S.A. Potekhin, E.L. Kovrigin, Folding under inequilibrium conditions as a possible reason for partial irreversibility of heat-denatured proteins: computer simulation study, Biophys. Chem. 73 (1998) 241–248.
[21] P.L. Privalov, Stability of proteins: small globular proteins, Adv. Protein Chem. 33 (1979) 167–241.
[22] B. Chen, J. King, Thermal unfolding pathway for the thermostable P22 tailspike endorhamnosidase, Biochemistry 30 (1991) 6260–6269.
[23] B.L. Chen, W.A. Baase, J.A. Schellman, Low-temperature unfolding of a mutant of phage T4 lysozyme. 2. Kinetic investigations, Biochemistry 28 (1989) 691–699.
[24] S. Segawa, M. Sugihara, Characterization of the transition state of lysozyme unfolding. I. Effect of protein–solvent interactions on the transition state, Biopolymers 23 (1984) 2473–2488.
[25] P.L. Privalov, N.N. Khechinashvili, A thermodynamic approach to the problem of stabilization of globular protein structure: a calorimetric study, J. Mol. Biol. 86 (1974) 665–684.
[26] A.I. Dragan, S.A. Potekhin, A. Sivolob, M. Lu, P.L. Privalov, Kinetics and thermodynamics of the unfolding and refolding of the three-stranded alpha-helical coiled coil, Lpp-56, Biochemistry 43 (2004) 14891–14900.
[27] A.E. Lyubarev, B.I. Kurganov, Modeling of irreversible thermal protein denaturation at varying temperature. I. The model involving two consecutive irreversible steps, Biochemistry (Mosc.) 63 (1998) 434–440.